21st AIAA Computational Fluid Dynamics Conference, 24–27 June 2013, San Diego, CA

Optimal Accuracy of Discontinuous Galerkin for Diffusion

Loc Khieu[*], Bram van Leer[†]

Department of Aerospace Engineering

University of Michigan

`khieuhl@umich.edu, bram@umich.edu`

and

Marcus Lo[‡]

`lo.marcus@gmail.com`

Abstract

The Recovery-based Discontinuous Galerkin method (RDG) for linear diffusion-shear problems is shown on triangles to achieve the order of accuracy $2p + 2$ for even p and $2p$ for odd p, where $p \geq 1$ is the order of the polynomial basis used. The RDG method incorporates a solution-enhancement step that reuses the recovery results, and an extra recovery step based on the enhanced solution. Thus, the stencil is extended not only to an element's face-sharing neighbors but also to the vertex-sharing ones. The order-of-accuracy results are obtained with Fourier analysis on a grid of structured right triangles.

I.   Introduction

The Discontinuous Galerkin (DG) method was originally developed for advection-type operators, for which it is pre-eminently suited,[1] but soon got applied to diffusion operators because of the need to model advection-diffusion processes with one numerical strategy. DG, however, is not naturally suited for diffusion operators, precisely because of the discontinuous solution representation, and requires a special step to overcome this handicap. Most of the newer methods require rewriting the second-order differential operator as a system of first-order operators, in order to arrive at a stable and accurate approximation.[2] In recovery-based

---

[*]Postdoctoral Fellow, member AIAA

[†]Professor, Fellow AIAA

[‡]Ph.D., Hong Kong, member AIAA

American Institute of Aeronautics and Astronautics

DG (RDG) a smooth solution basis, weakly identical to the discontinuous basis, is introduced for computing diffusive fluxes.[3]

We may pose the following question: *for a given order p of the elemental polynomial basis, what is the maximum order of accuracy DG can reach for diffusion-shear, if we allow only the direct neighbors of an element to participate in the discretization?* The answer is only known in part. On a Cartesian grid, which brings out the best in all DG methods, RDG has been demonstrated to achieve the order $3p+2$ or $3p+1$ for p even or odd, respectively;[4] this is the highest order found so far among DG schemes for diffusion. The result is robust: it holds in any number of dimensions, for nonlinear equations and equations with mixed derivatives, provided that

1. a tensor-product basis is used for the solution (sufficient for linear diffusion);

2. solution enhancement,[5] a technique of weak interpolation from element boundary to interior, is used to improve the volume integral in the DG equation for nonlinear diffusion;

3. an extra recovery step is used to improve the element-boundary integral in the presence of shear.

Lo[6,5] was the first to show the optimal accuracy for a 2-D diffusion-shear operator and for the 2-D Navier-Stokes terms; Varadan et al.[7] showed it for 3-D turbulence calculations.

When the tensor-product basis is abandoned for a lean basis of order p, the resulting order of RDG for diffusion on a Cartesian grid, with solution enhancement but without the extra recovery step, reduces to $2p + 2$,[8] which is still attractive. On simplex elements one can not maintain a tensor basis anyway, so we expect that on unstructured triangular or tetrahedral grids the order barrier is at best $2p+2$. Most DG methods for diffusion, including basic RDG-1x, reduce to the maximal order of accuracy $p + 1$ even on a structured grid of orthogonal triangles; only Hybrid DG (HDG)[9] has been shown to yield $p + 2$, owing to the use of independent face data.

In the present paper we describe our efforts to extend to a triangular grid those RDG techniques that yield the optimal accuracy on a 2-D Cartesian grid. Our structured grid of right triangles, shown in Figure 1 allows a Fourier analysis to find the exact order of accuracy of the DG discretization. It turns out that *RDG-1x++ achieves an accuracy of the order $2p+2$ or $2p$ for even or odd p, respectively, when simulating the linear diffusion-shear equation*, very close to our prediction.

As is always the case with RDG schemes, the key issues to be addressed are

1. what basis to choose in an element for the enhanced solution;

2. how to balance the number of basis functions of the enhanced solution with the number of conditions available at the faces.

After many trials and errors we arrived at one reformulation of the enhancement equations that avoids basis expansion, and another one in which the basis always expands by one order; the latter formulation may be preferred when solving problems that are nonlinear or governed by a system of equations.
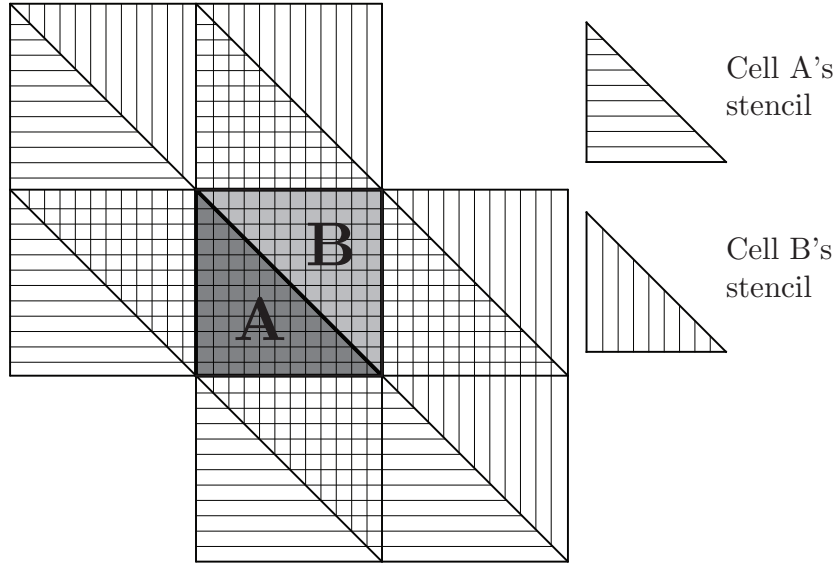
American Institute of Aeronautics and Astronautics

Figure 1. The stencil for Fourier analysis is the union of the stencils used for updating the triangles A and B which together form a square element of the underlying Cartesian grid.

II.   Recovery and Discontinuous Galerkin

We briefly review the formulation of RDG schemes for linear diffusion-shear in two dimensions. There are two basic versions of RDG: RDG-2x and RDG-1x. RDG-2x starts from a weak form of the diffusion-shear equation,

$$U_t = \nabla \cdot G(U), \tag{1}$$

$$G(U) = D\left\{ \begin{pmatrix} U_x \\ U_y \end{pmatrix} + \frac{\alpha}{2} \begin{pmatrix} U_y \\ U_x \end{pmatrix} \right\}, \tag{2}$$

obtainable after multiplication with a test function and integration by parts *twice* over the interior of an element Ω_j with boundary $\partial\Omega_j$:

$$
\iint\limits_{\Omega_j} (v_k)_j U_t d\Omega = \oint\limits_{\partial\Omega_j} (v_k)_j G(U) \cdot \hat{n} \, d\partial\Omega - \oint\limits_{\partial\Omega_j} U G(v_k)_j \cdot \hat{n} \, d\partial\Omega
$$

$$
+ \iint\limits_{\Omega_j} U \nabla \cdot G(v_k)_j d\Omega, \quad k = 1, ..., K(p), \ K(p) = (p+1)(p+2)/2. \tag{3}
$$

Here U is the true solution, D is a constant scalar diffusion coefficient and the $(v_k)_j$ are the basis/test functions spanning the 2-D polynomial space of order p on Ω_j and being zero elsewhere.

In a DG method U is replaced in the above equation by a numerical approximation u that in each element lies in the span of the basis $\{v_k\}$. This numerical solution is discontinuous at $\partial\Omega_j$; in RDG a unique interface value f is "recovered" by weakly interpolating between

American Institute of Aeronautics and Astronautics

the two abutting elements. For neighbors Ω_j and Ω_{j+1} the recovery equations are:

$$\iint_{\Omega_j} (v_k)_j f_{j,j+1} d\Omega = \iint_{\Omega_j} (v_k)_j u\, d\Omega, \quad k = 1, ..., K(p), \tag{4}$$

$$\iint_{\Omega_{j+1}} (v_k)_{j+1} f_{j,j+1} d\Omega = \iint_{\Omega_{j+1}} (v_k)_{j+1} u\, d\Omega, \quad k = 1, ..., K(p); \tag{5}$$

for details about the space in which $f_{j,j+1}$ is defined see.[8]

The RDG-2x scheme thus becomes:

$$\iint_{\Omega_j} (v_k)_j u_t d\Omega = \oint_{\partial\Omega_j} (v_k)_j G(f) \cdot \hat{n}\, d\partial\Omega - \oint_{\partial\Omega_j} f G(v_k)_j \cdot \hat{n}\, d\partial\Omega$$
$$+ \iint_{\Omega_j} u \nabla \cdot G(v_k)_j d\Omega, \quad k = 1, ..., K(p). \tag{6}$$

This scheme achieves the order of accuracy $2p + 2$ on Cartesian grids and $2p$ on triangular grids.

RDG-1x is obtained from the weak form integrated by parts once by again replacing U in the boundary integral with f:

$$\iint_{\Omega_j} (v_k)_j u_t d\Omega = \oint_{\partial\Omega_j} (v_k)_j G(f) \cdot \hat{n}\, d\partial\Omega - \iint_{\Omega_j} \nabla(v_k)_j \cdot G(u) d\Omega, \quad k = 1, ..., K(p). \tag{7}$$

This scheme achieves only $p + 1$ as its possible maximal order of accuracy regardless of grid type. Expanding the volume integral reveals the difference with RDG-2x:

$$\iint_{\Omega_j} (v_k)_j u_t d\Omega = \oint_{\partial\Omega_j} (v_k)_j G(f) \cdot \hat{n}\, d\partial\Omega - \oint_{\partial\Omega_j} u G(v_k)_j \cdot \hat{n}\, d\partial\Omega$$
$$+ \iint_{\Omega_j} u \nabla \cdot G(v_k)_j d\Omega, \quad k = 1, ..., K(p). \tag{8}$$

The second boundary integral is seen to contain u, that is, the boundary value in the interior of Ω_j, rather than the more accurate f, as in RDG-2x; this explains the plunge in accuracy.

Since it is not feasible to use RDG-2x for nonlinear problems, our strategy has been to develop solution-enhancement techniques for use in RDG-1x, so that the scheme becomes identical to RDG-2x in the linear case, then check numerically to what extent the latter's superconvergence property carries over to the nonlinear case. We therefore introduce an "enhanced" solution $\hat{u}$ to be used instead of u on the right-hand side of Eqn. (8), and require that the enhanced scheme RDG-1x+ be identical to RDG-2x:

$$-\oint_{\partial\Omega_j} \hat{u} G(v_k)_j \cdot \hat{n}\, d\partial\Omega + \iint_{\Omega_j} \hat{u} \nabla \cdot G(v_k)_j d\Omega$$
$$= -\oint_{\partial\Omega_j} f G(v_k)_j \cdot \hat{n}\, d\partial\Omega + \iint_{\Omega_j} u \nabla \cdot G(v_k)_j d\Omega, \quad k = 1, ..., K(p). \tag{9}$$

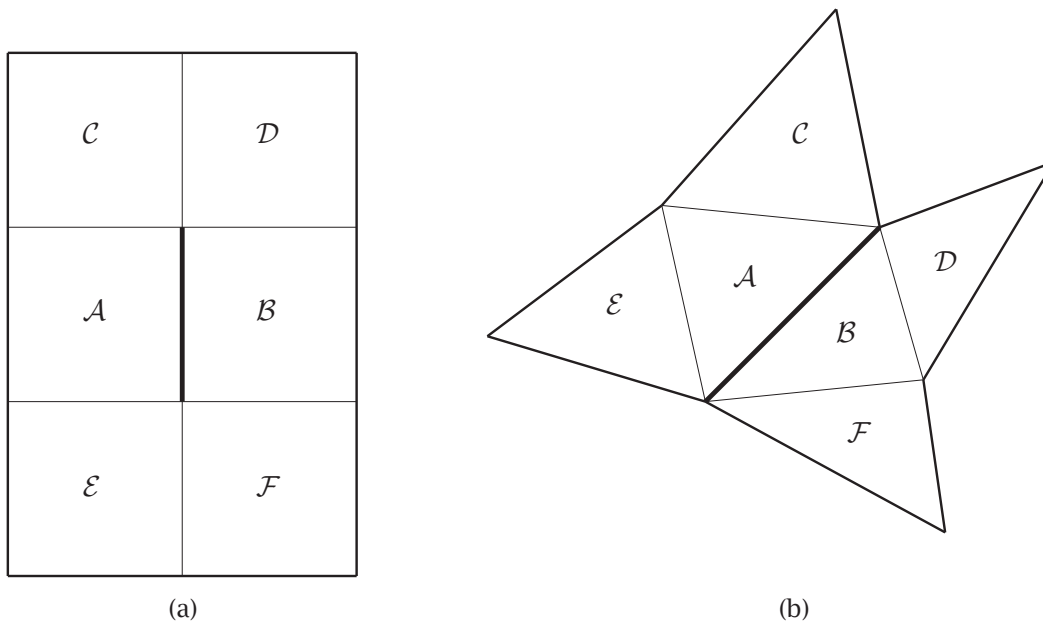American Institute of Aeronautics and Astronautics

Figure 2. Domain of dependence of recovered interface solution after the second recovery step, for (a) the most compact Cartesian scheme RDG-1x++CO (see[5]), (b) RDG-1x++ on a triangular grid (description in text).

In our earlier work, inspired by our experience on Cartesian grids, we would try to satisfy these equations by adding to u some higher-order polynomials that are to be orthogonal to the basis of u, so that the first $K(p)$ coefficients of $\hat{u}$ would be the same as the coefficients of u. To find their coefficients, these higher-order polynomials would share some weak properties with f on the boundary, e. g. the overall average value, or the average value on each individual face. This amounts to enhancing u by weak interpolation using information from neighbors, as in a finite-volume code. The name of the game is matching the number of added basis functions to the number of conditions on the boundary. In the next section we shall pursue this game more systematically.

Provided $\hat{u}$ is available, we can repeat the recovery step upon $\hat{u}$ to generate a smooth function $\hat{f}$ on the union of neighboring cells. Then, on the left-hand side of Eqn. (7), f and u are replaced by $\hat{f}$ and $\hat{u}$, respectively, to form the RDG-1x++ scheme.

A side effect of the latter step is that the computational stencil is enlarged. Figure 2(b) shows the domain of dependence in calculating $\hat{f}$ at the interface of cells $\mathcal{A}$ and $\mathcal{B}$; since $\hat{f}$ depends on $\hat{u}$ in $\mathcal{A}$ and $\mathcal{B}$, it depends on u in cells $\mathcal{C}$, $\mathcal{D}$, $\mathcal{E}$ and $\mathcal{F}$. Thus, the stencil is enlarged by the second recovery but does not go beyond the ring of cells around $\mathcal{A}$ that share at least a point with $\mathcal{A}$. The full stencil for updating one triangle is illustrated in Figure (3).

III.   Counting equations and basis functions

When developing RDG schemes for triangular elements we encountered three different procedures for satisfying the system of equations Eqn. (9); these are presented below (not in order of discovery!).

1. Equate the *sum* of the boundary integral and volume integral on the left-hand side to the *sum* of these integrals on the right-hand side. At first sight this yields $K(p)$ equations for the coefficients of the basis functions that build $\hat{u}$; the first equation,

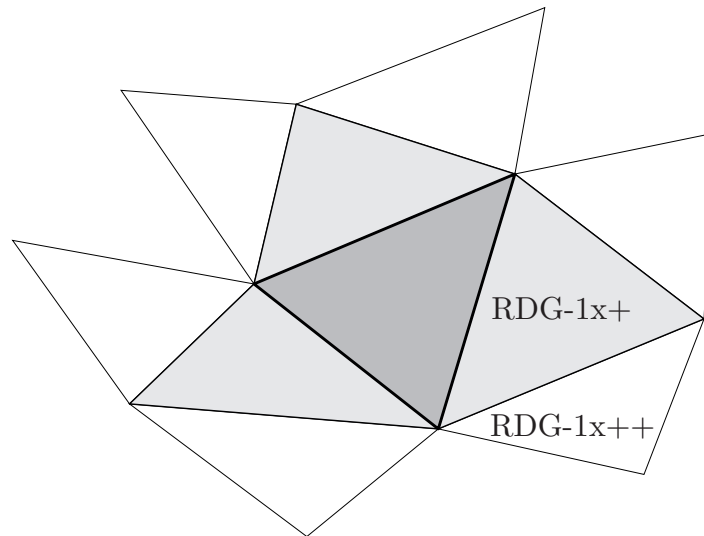American Institute of Aeronautics and Astronautics

Figure 3. Overall stencil of RDG-1x+ and RDG-1x++. RDG-1x+ uses only face-sharing neighbors, RDG-1x++ also uses the neighbors of these neighbors.

however, with $v_1 = 1$, gives no information as it reduces to $0 = 0$. Instead, we may introduce a conservation principle,

$$\iint\limits_{\Omega_j} \hat{u} \, d\Omega = \iint\limits_{\Omega_j} u \, d\Omega, \tag{10}$$

so that the number of equations is restored to $K(p)$; thus, the basis of $\hat{u}$ remains the same as that of u. This clearly is the most attractive way of satisfying Eqn. (9) if the flux $G(u)$ is linear; whether this procedure can be extended to the case of a nonlinear system without loss of accuracy remains to be investigated.

2. The boundary integrals and volume integrals on the left- and right-hand sides are matched *separately*. At first sight this leads to $2K(p)$ equations, which calls for enlargement of the solution basis. (NB: this does not mean an increase of the number of DG update equations; the enhancement is merely an *interpolation* process.) Closer inspection reveals that equating the boundary integrals yields $K(p) - 1$ equations, while matching the volume integrals has the equation count $K(p-2)$ of a basis of order $p-2$, because of the uniform second derivatives in the weight $\nabla \cdot G(v)$. The equation count thus becomes $(p+1)(p+2)/2 - 1 + (p-1)p/2 = p(p+1)$. When comparing this number to $K(p) = (p+1)(p+2)/2$, the number of basis functions in the span of u, we see that up to $p = 2$ the number of equations does not exceed $K(p)$, which means the original basis can be maintained provided that a solvable system of equations for the coefficients of $\hat{u}$ can be formulated. For $2 < p \le 4$ the number of equations does not exceed $K(p+1)$, meaning that the basis must be enlarged to one of order $p+1$. Increasing p further, a basis of order $p+2$ suffices up to $p = 6$ and a basis of order $p+3$ up to $p = 8$. The growth of the basis of $\hat{u}$ with increasing p is an unattractive feature of this procedure. It was the first thing we tried and it took considerable time and effort to come up with something more efficient.

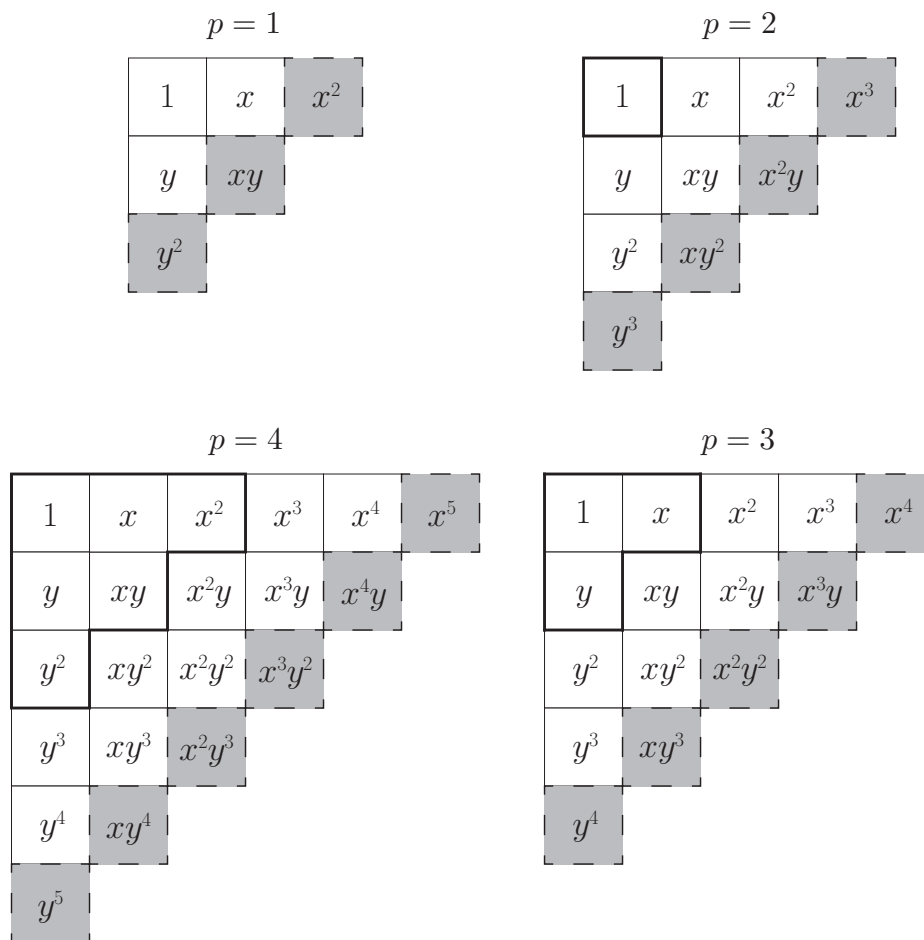3. There is a way of equating the boundary integrals that greatly reduces the equation

American Institute of Aeronautics and Astronautics

$p = 1$

1	x	x^2
y	xy	
y^2		

$p = 2$

1	x	x^2	x^3
y	xy	x^2y	
y^2	xy^2		
y^3			

$p = 4$

1	x	x^2	x^3	x^4	x^5
y	xy	x^2y	x^3y	x^4y	
y^2	xy^2	x^2y^2	x^3y^2		
y^3	xy^3	x^2y^3			
y^4	xy^4				
y^5					

$p = 3$

1	x	x^2	x^3	x^4
y	xy	x^2y	x^3y	
y^2	xy^2	x^2y^2		
y^3	xy^3			
y^4				

Figure 4. Monomial bases for enhanced interior solution $\hat{u}$ used in RDG-1x+ and RDG-1x++ on triangles, for $p = 1, 2, 3, 4$. The $p + 2$ polynomials of the order $p + 1$ that enhance the original basis of order p are bounded by dashed squares with interior shading; elements bounded by the thick solid line define *necessary* common moments between $\hat{u}$ and the original numerical solution u.

count: matching the contribution to the integrals at each individual face. Consider one such face and switch to a coordinate system (r, s) aligned with it; that is, r measures distance normal to the face ($r = 0$ on the face), s along the face. (NB: This is the frame in which also f is obtained.) The segment of the boundary integral along this face provides p pieces of information about $\hat{u}$ or f: in essence the face integrals of the solution weighted with the facial test functions $1, s, ..., s^{p-1}$. (The weight s^p is absent because the weight $G(v)$ contains only first derivatives.) Without changing the way of matching the volume integrals we now end up with a total equation count of $3p + p(p - 1)/2 = p(p + 5)/2$. This is always greater than $K(p)$ for $p \geq 1$, but less than $K(p + 1)$, the difference being $(p + 2)(p + 3)/2 - p(p + 5)/2 = 3$ for any p. This suggests adding

- one extra constraint at each face by, for instance, matching the face integrals of $\partial \hat{u}/\partial r$ to $\partial f/\partial r$ (the resulting schemes are denoted by RDG-1x+b and RDG-1x++b); or

- three constraints on the pair of volume integrals by matching three higher-order moments of $\hat{u}$ to those of u. These moments are in addition to the ones already

American Institute of Aeronautics and Astronautics

p	Additional moment weights		
1	1	x	y
2	x	y	$\frac{1}{3}\left(x^2 + y^2 + xy\right)$
3	x^2	y^2	xy
4	x^3	y^3	$\frac{1}{2}\left(x^2 y + xy^2\right)$

Table 1. Weights in the moments defining three additional constraints on the volume integral as discussed in Section III.

defined in $\nabla \cdot G\left(v\right)$, represented by the elements within the thick solid bound in Figure (4) for $1 \leq p \leq 4$. The resulting schemes are temporarily denoted by RDG-1x+v and RDG-1x++v. Examples of weight functions for $p \leq 4$ are shown in Table 1.

The number of equations now also equals $K(p + 1)$ and, for these particular choices, the system is solvable for all p, even or odd. Eqn. (9) has been satisfied by increasing the order of the solution basis by only 1, for all p; that is, $p + 2$ basis functions are to be added to the original $(p + 1)(p + 2)/2$, as illustrated by Figure (4) for p up to 4. (NB: we skip the degenerate case $p = 0$, in which Eqn. (9) reduces to 0=0.) This is the most efficient procedure that we judge suitable for nonlinear systems.

In the next section we show the results of our Fourier analysis on the right-triangle grid of Figure (1).

IV.   Results of Fourier analysis

Our order-of-accuracy analysis of various linear spatial DG operators is carried out entirely with Mathematica. Our frequency variables are $\beta_x = 2\pi\Delta x/l_x$ and $\beta_y = 2\pi\Delta y/l_y$, where l_x and l_y are the wavelengths of the Fourier modes in the x- and y-direction. To simplify the analysis we assume $\beta_x = \beta_y = \beta$, $\Delta x = \Delta y = \Delta$, making the analysis one-dimensional; in our experience with advection-diffusion-shear DG schemes, the order of accuracy found for these coupled frequencies is always indicative of the order found from the full 2-D analysis.

We make the DG scheme nondimensional by multiplying both sides with Δ^2/D, then we determine the Fourier transform of the spatial operator. Next we determine the equation for its eigenvalues; there are $K(p)$ of these but we are only interested in the one consistent with the operator for $\beta \to 0$ (the "good" eigenvalue, see[1]); we'll call this value λ_{co}. The transform of the nondimensionalized spatial operator in the original PDE (1) is

$$\lambda_{ex} = -(2 + \alpha)\beta^2; \tag{11}$$

the value of λ_{co} is produced by Mathematica in the form of a Taylor series, of which the leading term should be λ_{ex}. Thus, we produce the eigenvalues and select the one with the proper leading term.

As an example, consider RDG-2x for $p = 1$. We analyze the operator on the combination of two cells A and B, each with 3 unknowns, leading to a 6×6 matrix operator; this is

American Institute of Aeronautics and Astronautics

p	RDG-2x OOA	RDG-1x OOA	RDG-1x+v/b OOA	RDG-1x++b OOA	RDG-1x++v OOA
1	2	2	2	2	2(4 when $\alpha = 1$)
2	4	2	4	4	6
3	6	4	6	6	6
4	8	4	8	8	10

Table 2. Order of accuracy (OOA) of various linear RDG schemes up to $p = 4$ in approximating Eqn. (1).

displayed below, for $\alpha = 1$.

$$M(\beta) =$$

$$\begin{pmatrix}
-30 & -2 & -3 & 18 + 12e^{-i\beta} & \frac{3}{2} + \frac{e^{-i\beta}}{2} & \frac{9}{4} + \frac{3e^{-i\beta}}{4} \\
-36 & -\frac{405}{8} & \frac{15}{8} & 27 + 9e^{-i\beta} & -\frac{333}{16} + \frac{3e^{-i\beta}}{16} & \frac{441}{32} - \frac{381e^{-i\beta}}{32} \\
-72 & \frac{5}{2} & -\frac{385}{8} & 54 + 18e^{-i\beta} & \frac{147}{8} - \frac{127e^{-i\beta}}{8} & -\frac{39}{16} - \frac{251e^{-i\beta}}{16} \\
18 + 12e^{i\beta} & \frac{3}{2} + \frac{e^{i\beta}}{2} & \frac{9}{4} + \frac{3e^{i\beta}}{4} & -30 & -2 & -3 \\
27 + 9e^{i\beta} & -\frac{333}{16} + \frac{3e^{i\beta}}{16} & \frac{441}{32} - \frac{381e^{i\beta}}{32} & -36 & -\frac{405}{8} & \frac{15}{8} \\
54 + 18e^{i\beta} & \frac{147}{8} - \frac{127e^{i\beta}}{8} & -\frac{39}{16} - \frac{251e^{i\beta}}{16} & -72 & \frac{5}{2} & -\frac{385}{8}
\end{pmatrix}. \quad (12)$$

The consistent eigenvalue is given by the following series:

$$\lambda_{co}(\beta) = -3\beta^2 + \frac{13\beta^4}{272} + \frac{939\beta^6}{369920} + \frac{4179319\beta^8}{6338949120} + O\left(\beta^{10}\right), \quad (13)$$

indicating second-order accuracy. As another example of the same analysis we take $p = 3$; due to its large size (20×20) matrix is not displayed. Only its consistent eigenvalue is given below, illustrating a sixth-order accuracy:

$$\lambda_{co}(\beta) = -3\beta^2 + 1.127 \times 10^{-5}\beta^8 + 1.724 \times 10^{-6}\beta^{10} + O\left(\beta^{12}\right). \quad (14)$$

The results for five RDG schemes (RDG-1x+v and RDG-1x+b are identical in the linear case) and four values of p are summarized in Table 2. It is seen that RDG-2x is accurate to the order $2p$, while RDG-1x shows a staircase-like progression of its order, that is, $p + 1$ for odd p, and $p(!)$ for even p. The enhancements in RDG-1x+v/b and RDG-1x++b restore the accuracy of the integration-by-parts-once formulation to the level of RDG-2x; surprisingly, the RDG-1x++v scheme manages to raise the order for even p further to $2p + 2$ from $2p$.

V.   Conclusions and future work

We have extended the Recovery-based Discontinuous Galerkin method RDG-1x++, which on a Cartesian grid gives optimal accuracy, to a grid of triangles, for solving linear diffusion-shear problems. In doing so, the order of accuracy is observed to drop from $2p + 2$ on rectangles to $2p$ on triangles only for odd value of p.

Scheme RDG-1x++ involves two solution enhancements: interior-solution enhancement and recovered-function enhancement. For the former, we develop two practical procedures:

American Institute of Aeronautics and Astronautics

one in which the solution basis need not be enlarged, another one in which the solution basis is enlarged by one polynomial order. The enhancement is an interpolation step and does not lead to an increase in the number of DG update equations. For the latter enhancement, the recovery step is applied again upon $\hat{u}$, obtained from the first enhancement step, to produce a smooth function $\hat{f}$. It is used in the boundary integral to improve its accuracy. A side effect of the second enhancement is the enlargement of the stencil to include some neighbors sharing at least a point with the updated cell.

Two obvious further extensions are considered for the future.

1. *Linear extension.* A second interior-solution-enhancement step, yielding a solution $\hat{\hat{u}}$, would potentially further enhance the accuracy of the operator, while the domain of dependence would not be further affected.

2. *Nonlinear extension.* The greatest challenge is to make the RDG-1x+ and RDG-1x++ schemes suitable for nonlinear diffusion-shear systems on triangular grids, without loss of accuracy. This task is far from trivial, but the complete success in the case of Cartesian grids gives us confidence in its future completion. We do believe that Option 3 of Section III, particularly RDG-1x++v flavor, will turn out to be the best path to nonlinear extension, as this option offers more flexibility than Option 1, and with better accuracy.

Acknowledgements

American Institute of Aeronautics and Astronautics

References

[1]B. van Leer and S. Nomura, "Discontinuous Galerkin for diffusion," AIAA Paper 2005-5108, 2005.

[2]B. Cockburn and C.-W. Shu, "The Local Discontinuous Galerkin method for time-dependent convection-diffusion systems," *SIAM Journal on Numerical Analysis*, vol. 35, pp. 2440–2463, 1998.

[3]B. van Leer and M. Lo, "Unification of Discontinuous Galerkin methods for advection and diffusion," AIAA Paper 2009-0400, 2009.

[4]M. Lo and B. van Leer, "Analysis and implementation of the Recovery-based Discontinuous Galerkin method for diffusion," AIAA Paper 2009-3786, 2009.

[5]M. Lo and B. van Leer, "Recovery-based discontinuous Galerkin for Navier-Stokes viscous terms," AIAA Paper 2011-3406, 2011.

[6]M. Lo, *A Space-Time Discontinuous Galerkin Method for Navier-Stokes witth Recovery.* PhD thesis, University of Michigan, 2011.

[7]S. Varadan, E. Johnsen, and B. van Leer, "A three-dimensional recovery-based Discontinuous Galerkin method for turbulence simulations," AIAA Paper 2013-0515, 2013.

[8]B. van Leer, M. Lo, and M. van Raalte, "A Discontinuous Galerkin method for diffusion based on recovery," AIAA Paper 2007-4083, 2007.

[9]J. Peraire, N. Nguyen, and B. Cockburn, "A hybridizable Discontinuous Galerkin method for the compressible euler and navier-stokes equations," AIAA Paper 2010-363, 2010.

American Institute of Aeronautics and Astronautics